



HAL
open science

CEST MRI at 7T using an optimized parallel transmission saturation scheme

Thaddée Delebarre, Vincent Gras, Franck Mauconduit, Alexandre Vignaud,
Nicolas Boulant, Luisa Ciobanu

► **To cite this version:**

Thaddée Delebarre, Vincent Gras, Franck Mauconduit, Alexandre Vignaud, Nicolas Boulant, et al.. CEST MRI at 7T using an optimized parallel transmission saturation scheme. ISMRM 2022 - Joint Annual Meeting ISMRM-ESMRMB & ISMRT 31st Annual Meeting, May 2022, Londres, United Kingdom. <hal-05121413>

HAL Id: hal-05121413

<https://hal.science/hal-05121413v1>

Submitted on 19 Jun 2025

HAL is a multi-disciplinary open access archive for the deposit and dissemination of scientific research documents, whether they are published or not. The documents may come from teaching and research institutions in France or abroad, or from public or private research centers.

L'archive ouverte pluridisciplinaire **HAL**, est destinée au dépôt et à la diffusion de documents scientifiques de niveau recherche, publiés ou non, émanant des établissements d'enseignement et de recherche français ou étrangers, des laboratoires publics ou privés.



Distributed under a Creative Commons CC0 1.0 - Universal - International License

2718

CEST MRI at 7T using an optimized parallel transmission saturation scheme

Thaddée Delebarre^{1,2}, Vincent Gras^{1,2}, Franck Mauconduit^{1,2}, Alexandre Vignaud^{1,2}, Nicolas Boulant^{1,2}, and Luisa Ciobanu^{1,2}
¹NeuroSpin, CEA, Saclay, France, ²Paris-Saclay University, Gif-sur-Yvette, France

Synopsis

Compared to the traditional circular polarization (CP) transmission mode, parallel transmission (pTx) excitation allows significant gains in contrast and homogeneity for Chemical Exchange Saturation Transfer (CEST) imaging. Using an in-house developed CEST-EPI sequence incorporating a pTx optimized CEST saturation block, we show that both tailored and universal pTx pulses provide significant improvement at 7T for APT-CEST, GlucoCEST and GlucoCEST imaging and enable saturation powers unattainable with CP.

Introduction

The use of Chemical Exchange Saturation Transfer (CEST) for the enhanced detection of various brain metabolites has been already demonstrated¹⁻³. To reduce artifactual spatial variations in the CEST contrast introduced by B_1^+ inhomogeneity, post processing algorithms^{4,5} or parallel transmission^{6,7} (pTx) solutions have been proposed. In this study, we use pTx at 7T to achieve a more intense and homogenous saturation than when using circular polarization (CP) while respecting the Specific Absorption Rate (SAR) constraints. Validated virtual observation points (VOPs) with the NOVA (Wilmington, MA, USA) pTx coil were employed to boost performance compared to the conservative power limits normally used ("protected" mode).

Materials and Methods

All measurements were performed on a 7T Magnetom Scanner (Siemens Healthcare, Erlangen, Germany) with the NOVA 8Tx-32Rx channels head coil using an in-house developed 2D-CEST-EPI sequence. The CEST saturation module was composed of two interleaved⁸ pTx pulses (Figure 1). The optimization of the pTx modes consisted in the minimization of least square error to a target B_1 rms under local SAR, global SAR and RF power limitations, using previously acquired B_1^+ maps. For all channels, the pulses were Hanning-windowed Gaussians of 50ms duration. VOPs included several safety factors⁹ while imposing power limits of 3W (per channel) and 16W (total).

Phantom and volunteer experiments

A realistic head phantom¹⁰ consisting of two compartments was filled with 10mM glucose (inner compartment) and 15mM creatine (outer compartment) in agarose. Both compartments contained 4g/L NaCl and 64 μ M gadolinium, for a relaxation time T_1 of 1600ms, and were adjusted to pH 7.0. Before the experiments, the phantom was warmed up to 37°C. For the *in vivo* investigations, 4 healthy volunteers were recruited after providing informed written consent. The study was approved by the local IRB.

CEST acquisitions

Single slice, 4mm thick, CEST images were acquired with an in-plane resolution of 3.4x3.4mm². Z-spectra were sampled with 41 saturation offsets from -5ppm to 5ppm and an additional one for reference at -10ppm. For *in vivo* experiments, circular polarization (CP), universal pulses¹¹ (UPs) and single subject Tailored pulses (TP) were tested. UPs were designed before the acquisition on a dataset consisting of B_1^+ maps from 15 individuals and were used as such whereas the TPs were designed using a B_1^+ map acquired using the interferometric turbo-FLASH method¹² at the beginning of the exam.

For GlucoCEST, the saturation module consisted of 20 pulses of 1.12s saturation duration and a target B_1 rms of 1.5 μ T. The maximum reachable B_1 rms in CP mode was 1.2 μ T on the imaged slice. For GlucoCEST, the saturation was made with 16 pulses of 0.9s total duration and a target B_1 rms of 3 μ T. In this case the maximum attainable B_1 rms was 1.7 μ T for the CP mode. GlucoCEST images were only acquired *in vivo*.

For each dataset, a low saturation acquisition was also performed and used for WASSR¹³ B0 correction (21 saturation offsets from -1ppm to 1ppm, mean B_1 rms=0.15 μ T).

Data analysis

Within slice motion and distortion correction was implemented using SPM12. Subsequently, the image series was B0 corrected and MTR_{asym} maps were calculated voxel by voxel according to

$$MTR_{asym}(\Delta\omega) = \frac{S(-\Delta\omega) - S(\Delta\omega)}{S_{ref}}$$

Results

Phantom results

Figure 2 shows simulated B1rms profiles for both CP and pTx-TP mode for a target mean B1rms of 1.5 μ T (A) and the measured GlucoCEST MTR_{asym} maps (B) on a transversal slice located +5mm from isocenter. The MTR_{asym} map obtained with the pTx-TP mode is more homogeneous than with CP, with a relative standard deviation across the slice of 13% vs 32%. In addition, the pTx-TP mode enables good CEST contrast at the borders of the brain, which is not the case for the CP mode. Figure 3 shows a comparison between Z-spectra obtained in two different ROIs using the CP and pTx-TP modes. The spectra acquired with pTx-TP mode are almost identical, as it is expected for a homogeneous phantom, whereas for CP, they are very different with a significant difference of the FWHM of water peak between the two ROIs (more than double).

In vivo results

Figure 4 presents GlucoCEST MTR_{asym} maps obtained with CP, pTx-UP and pTx-TP modes in which the benefits of pTx over CP are evident. For both UP and TP, saturation with a homogenous B1rms (relative STD of 8% and 4%, respectively compared to 18% for CP) leads to an increased contrast compared to CP. We notice that TPs present a slight contrast improvement as compared to UPs, not only between brain tissue and CSF but also between gray and white matter. Similar performance was also obtained for APT-CEST and GluCEST imaging. Figure 5 presents examples of GlucoCEST, GluCEST and APT-CEST MTR_{asym} maps fused with the anatomical image.

Discussion and conclusion

The use of pTx for CEST acquisitions provides more homogenous and contrasted images and allows levels of saturation not permitted with the CP mode. Compared to ref [6] our approach is simpler offering in the same time more flexibility than the development presented in [7]. Although the single subject tailored pulses perform slightly better than the universal pulses, the latter have the advantage of considerably simplifying the workflow while still significantly outperforming the CP mode.

Acknowledgements

We acknowledge funding from ANR (project fMETAMR) and Leducq Foundation (Large Equipment ERPT program, NEUROVASC7T project).

References

- [1] Yadav NN, Xu J, Bar-Shir A, et al. Natural D-glucose as a biodegradable MRI relaxation agent. *Magnetic Resonance in Medicine* 2014;72:823–828.
- [2] Cai K, Haris M, Singh A, et al. Magnetic resonance imaging of glutamate. *Nat Med* 2012;18:302–306.
- [3] Jones CK, Schlosser MJ, van Zijl PCM, et al. Amide proton transfer imaging of human brain tumors at 3T. *Magnetic Resonance in Medicine* 2006;56:585–592.
- [4] Windschuh J, Zaiss M, Meissner J-E, et al. Correction of B1-inhomogeneities for relaxation-compensated CEST imaging at 7 T. *NMR in Biomedicine* 2015;28:529–537.
- [5] Sun PZ, Farrar CT, Sorensen AG. Correction for artifacts induced by B0 and B1 field inhomogeneities in pH-sensitive chemical exchange saturation transfer (CEST) imaging. *Magnetic Resonance in Medicine* 2007;58:1207–1215.
- [6] Tse DHY, da Silva NA, Poser BA, et al. B1⁺ inhomogeneity mitigation in CEST using parallel transmission. *Magnetic Resonance in Medicine* 2017;78:2216–2225.
- [7] Liebert A, Tkotz K, Herrler J, et al. Whole-brain quantitative CEST MRI at 7T using parallel transmission methods and correction. *Magnetic Resonance in Medicine* 2021;86:346–362.

- [8] Liebert A, Zaiss M, Gumbrecht R, et al. Multiple interleaved mode saturation (MIMOSA) for B1+ inhomogeneity mitigation in chemical exchange saturation transfer. *Magnetic Resonance in Medicine* 2019;82:693–705.
- [9] Boulant N, Gras V, Amadon A, et al. (2018) ‘Workflow proposal for defining SAR safety margins in parallel transmission’, in *Proceedings of the 26th Annual Meeting of ISMRM*. Paris.
- [10] Jona G, Furman-Haran E, Schmidt R. Realistic head-shaped phantom with brain-mimicking metabolites for 7 T spectroscopy and spectroscopic imaging. *NMR in Biomedicine* 2021;34:e4421.
- [11] Gras V, Vignaud A, Amadon A, et al. Universal pulses: A new concept for calibration-free parallel transmission. *Magnetic Resonance in Medicine* 2017;77:635–643.
- [12] Amadon A, Cloos M, Boulant N, et al. Validation of a very fast B1-mapping sequence for parallel transmission on a human brain at 7 T. 2011. *In Proceedings of the 20th Annual Meeting of ISMRM*, p. 3358.
- [13] Kim M, Gillen J, Landman BA, et al. Water Saturation Shift Referencing (WASSR) for chemical exchange saturation transfer experiments. *Magn Reson Med* 2009;61:1441–1450.

Figures

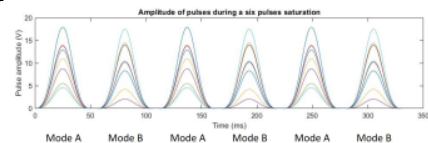


Figure 1 : Example of pulse amplitudes for a six pulse saturation module. Each color represents a different Tx-channel.

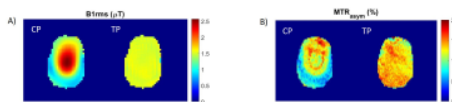


Figure 2: (A) CP (left) and pTx TP (right) simulated $B1_{rms}$ maps for a target mean $B1_{rms}$ of $1.5 \mu T$. (B) Measured GlucoCEST MTR_{asymp} ($\delta=1.25 \pm 0.25 ppm$) maps using the CP mode (left) and the pTx TP mode (right).

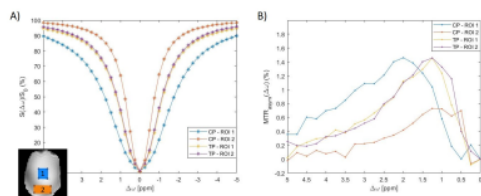


Figure 3: (A) Averaged Z-spectra over the blue and red ROIs obtained with the CP and pTx-TP modes and (B) corresponding MTR_{asymp} spectra.

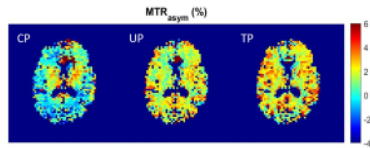


Figure 4: GlucoCEST MTR_{asym} ($\delta=1.25 \pm 0.25\text{ppm}$) maps for CP, pTx-UP and pTx-TP saturation modes.

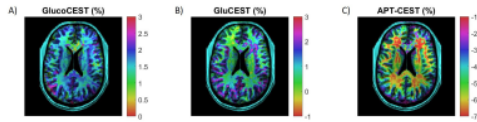


Figure 5: Fusion of (A) GlucoCEST ($\delta=1.25 \pm 0.25\text{ppm}$), (B) GluCEST ($\delta=3.0 \pm 0.25\text{ppm}$) and (C) APT-CEST ($\delta=3.5 \pm 0.25\text{ppm}$) MTR_{asym} maps with anatomical images acquired using pTx single subject TP. The MTR_{asym} maps were linearly interpolated to fit the resolution of the anatomical image. 2D-CEST-EPI parameters for GlucoCEST and APT-CEST: TR/TE=2500/34, CEST saturation module duration: 1.12s. For GluCEST: TR/TE=5000/34, CEST saturation module duration: 0.9s.